

Applications of Godiva II Neutron Pulses

By T. F. Wimett and J. D. Orndoff *

The production of self-limiting fission bursts initiated by a single large reactivity change was first demonstrated at the Los Alamos Scientific Laboratory with the bare spherical uranium metal critical assembly, "Lady Godiva" or Godiva I (Fig. 1), in 1953.¹ Following the completion of a program to determine properties of these bursts as functions of excess reactivity, there was an increasing demand for the use of Godiva I as an experimental tool in neutron pulse irradiation investigations. As a result, this experimental critical assembly was pressed into service as a fission burst facility and produced a total of ~ 1000 bursts before its retirement following an accidentally intense burst.² A large backlog of experimental programs necessitated the design and construction of Godiva II, which is similar to Godiva I except for differences in geometry arising from different functional requirements; Godiva II was designed specifically for the reliable production of super-prompt-critical fission bursts while its predecessor was not.

This paper presents some of the observed properties of fission bursts showing their relation to theory together with examples of a number of different experiments utilizing Godiva I and II bursts.

ASSEMBLIES

Figure 1 shows Godiva I in its disassembled state. As a bare enriched ($\sim 93.5\%$ U^{235}) uranium critical assembly for basic studies, it is described in detail in Ref. 1. When assembled, Godiva I was a slightly elongated sphere (~ 53 kg) $\sim 6\frac{3}{4}$ in. in diameter supported by tubular steel hangars (to minimize neutron reflection) and tubular drive rods for the upper and lower retractable sections. In addition to ~ 0.75 dollar of continuously variable

reactivity in two control rods, stepwise reactivity adjustment from 0.05 to ~ 1.0 dollar could be accomplished by attaching small uranium discs (~ 50 or ~ 100 g) in some of fourteen recesses on the surface. For burst operation, the assembly was modified by the addition of a uranium "burst rod" $\frac{1}{2}$ in. in diameter and 8 in. in length which could be inserted rapidly into the glory hole, a diametrical channel through the stationary middle section. Initially projecting about two inches into the glory hole, it could be fully inserted by means of an explosive charge or pneumatic cylinder.

Figure 2 is a photograph of Godiva II, showing the three-legged aluminum supporting structure which houses relay interlocks, pneumatic actuating devices, and local controls. Electrical control rod drives including selsyns for transmitting rod position information to the remote control point are visible on top of the tripod arrangement. Above these and inside a wire cage is the nickel-coated active material, with configuration details as shown in the sketch of Fig. 3. The major section is a ~ 7 -in.-diameter right circular cylinder, with a spherically-shaped top, and is solid with the exception of four cavities opening at the bottom surface. A coaxial cylindrical cavity accommodates the "safety block" which is a solid cylinder and is shown in its scrambled position. Because reliable shutdown depends largely on the easy withdrawal of this safety block, a clearance of 0.06 in. is provided between its surface and the cavity wall to prevent jamming. Two control rods and a burst rod also enter the main section from the bottom. Both the main section and the safety block are mounted on $\frac{3}{8}$ -in. steel plates by means of uranium bolts; the plates are supported by vertical steel rods. Steel rods also are threaded into the uranium control rods and burst rod to connect them through guides to actuating mechanisms—screws driven by electric motors for the control rods and a pneumatic cylinder for the burst rod. Pneumatic cylinders are also used to position the safety block and a Pu-Be neutron source which can be raised from a remote position to a position two inches from the assembly surface. The total mass of enriched uranium ($\sim 93.2\%$ U^{235}) is ~ 57.7 kg. Operation of assembly machinery is performed entirely by remote control at a distance of about $\frac{1}{4}$ mile to ensure personnel safety.

* Authors and contributors—P. C. Fisher, G. A. Graves, G. E. Hansen, P. S. Harris, G. R. Keepin, P. G. Koontz, J. D. Orndoff, H. C. Paxton, R. H. White and T. F. Wimett are with the University of California, Los Alamos Scientific Laboratory, Los Alamos, New Mexico; P. W. Levy, Brookhaven National Laboratory, Upton, L.I., New York; D. M. Newell, Convair, Fort Worth, Texas; H. J. Stein and others, Sandia Corporation, Albuquerque, New Mexico; J. W. Wachter, Union Carbide Nuclear Company (Y-12 Plant), Oak Ridge, Tennessee.

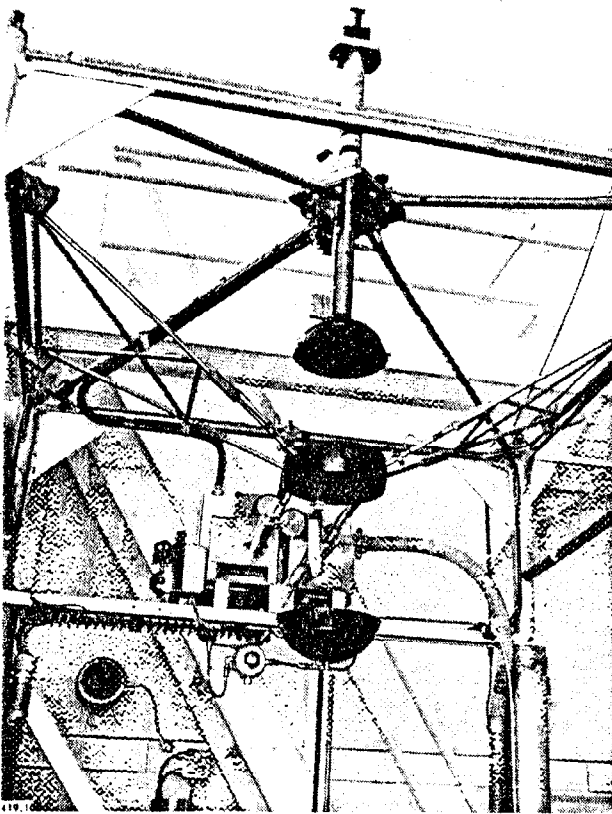


Figure 1. View of Godiva I in scrambled state showing hangar system with control rod mechanisms visible behind the central section

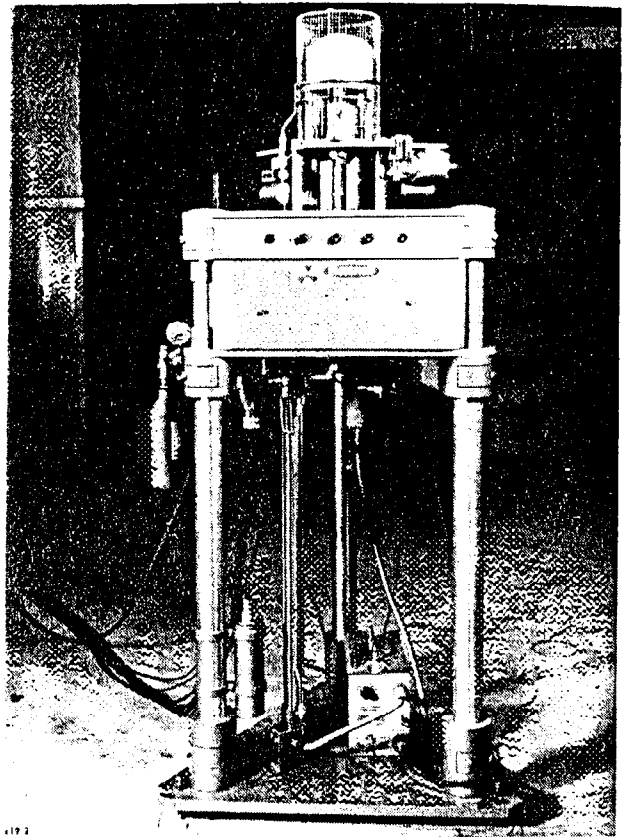


Figure 2. View of Godiva II in scrambled state with nickel-clad active material visible inside cage at top of assembly machinery

Features of Godiva II leading to improved performance as a burst irradiation facility are:

1. Easy access for irradiations. Irradiation of small central samples can be done by means of a sample transfer tube passing through the assembly. The space around and above the assembly is essentially unimpeded, except for the wire cage shown in Fig. 2, which prevents the placing of any neutron-reflecting material in such proximity as to cause excessive reactivity perturbation.

2. Rigid mechanical mounting which provides good reproducibility.

3. Nickel cladding on exposed uranium surfaces. This prevents surface oxidation, which is not only a health hazard but also may interfere with reproducible seating of assembly components.

4. Massive control rods (2.3 dollars reactivity control). These permit necessary mass adjustments (to correct for neutron reflection from samples near the cage, for example) to be done entirely by remote control. (Manual adjustment with the surface discs on Godiva I often led to excessive personnel radiation exposure.)

5. Forced air cooling. This comes from a manifold on the cage and serves to minimize the wait time between bursts.

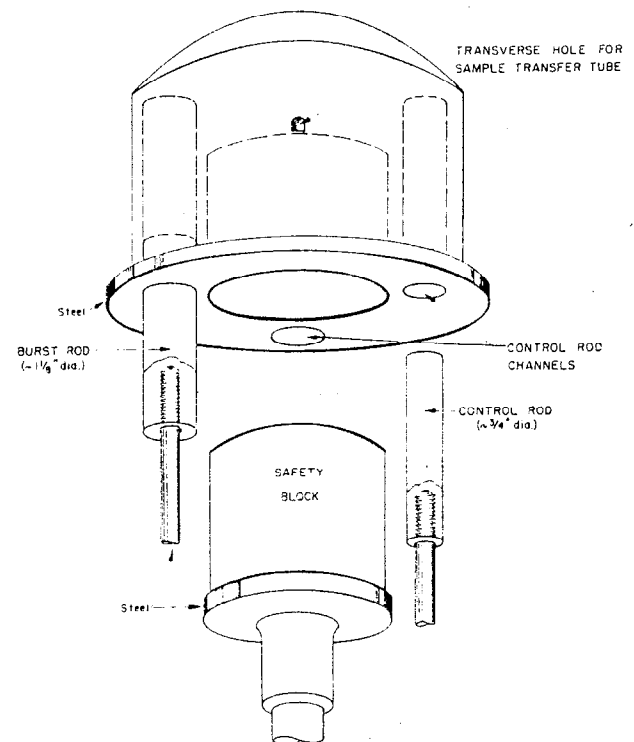


Figure 3. Drawing of Godiva II showing safety block and control rods which enter main section from below

6. Compact machine size and portability. Permits flexible operation.

7. Electrical interlocks to control burst generation procedure. These require a correct, safe, starting sequence before the burst rod can be actuated.

8. Isolation of central mass in the safety block. This not only makes withdrawal of the safety block most effective as a shutdown device but also tends to reduce the effects of thermal shock accompanying a burst by providing for free expansion of the central, hotter, section into the oversized cavity without transmitting strain to the assembly surface.

BURST GENERATION

Under controlled conditions, a fission burst is generated by the sudden assembly of a supercritical configuration provided the act of assembly is completed before buildup of an appreciable neutron population. For predictable yields, it is also necessary that the excess reactivity of the final configuration be known to considerable accuracy. The procedure followed on Godiva I and II which is consistent with these requirements is first to make an assembly with the burst rod retracted and the neutron source in position near the active material. The control rods are adjusted for steady power at some arbitrary low level thus establishing a "delayed critical" configuration. Next, the safety block of Godiva II, or upper section of Godiva I, and the neutron source are retracted leaving the control rods in position and the neutron population is allowed to decay. Upon reinserting the safety block and then inserting the burst rod (its out-position is chosen by previous calibration; insertion involves shifting from there to ~ 0.015 in. of seating), a known final reactivity in the vicinity of prompt critical is attained. Different final reactivities are obtained by readjusting a control rod immediately before burst rod insertion.

The prompt fission burst is automatically limited by thermal expansion but there persists a residual power level sustained by delayed neutron activity, as discussed in the next section. Because this residual level produces a temperature rise of $\sim 100^\circ\text{C}$ per second, it is desirable to scram the assembly as rapidly as possible. For this purpose, a special "fast-scram" system was devised by which a radiation-level trigger-pulse closes a solenoid air valve and applies pressure to the air piston which withdraws the safety block. Scram time achieved in this way is ~ 0.04 second. For safety, there are additional standard independent scram circuits connected to radiation monitors.

STUDIES OF BURST PROPERTIES

Theoretical

The space-averaged one-velocity neutron transient equation³ for a fast assembly is

$$\frac{\dot{n}(t)}{\alpha_R} = \rho(t)n(t) + \sum_{i=1}^6 a_i \lambda_i \int_{-\infty}^t e^{-\lambda_i(t-\xi)} n(\xi) d\xi \quad (1)$$

where $\dot{n}(t)$ is the time derivative of space-averaged neutron density $n(t)$; α_R is a decay constant which can be associated with fission chain decay at delayed critical⁴; $\rho(t) \equiv (K_p - 1)/K_p \gamma \beta$, is excess reactivity measured in dollars from prompt critical, K_p is the prompt neutron reproduction number and

$\gamma \beta \equiv \sum_{i=1}^6 \gamma_i \beta_i$, is averaged delayed neutron effective abundance relative to prompt neutrons; $a_i \equiv \gamma_i \beta_i / \gamma \beta$, is the effective relative abundance of the i th delayed neutron group and λ_i , γ_i , β_i are, respectively, the decay constant, relative effectiveness and group fraction of the i th group. An underlying assumption in Eq. (1) is that the neutron mean life for fission is time independent. The maximum error introduced by this assumption would be $\sim 1\%$ for a total reactivity change (from thermal expansion, for example) of one dollar which is greater than any considered herein.

The solution of Eq. (1) for fission bursts is simplified if reactivity is assumed to decrease linearly with fission energy release as a result of thermal expansion,[†] i.e., $\rho(t) = \rho_0 - F(t)$ where ρ_0 is the initial reactivity and $F(t)$ is total fissions in reactivity units. (Experimentally, the energy from 4.8×10^{16} fissions reduces reactivity by one dollar in Godiva I.) Rewriting Eq. (1) with this expression for $\rho(t)$ and replacing neutron density $n(t)$ by fission rate $\dot{F}(t)$ (in dollars per second) which is directly proportional to it yields

$$\frac{\ddot{F}}{\alpha_R} = [\rho_0 - F(t)]\dot{F}(t) + \sum_{i=1}^6 a_i \lambda_i \int_{-\infty}^t e^{-\lambda_i(t-\xi)} \dot{F}(\xi) d\xi \quad (2)$$

While a solution to this equation governing the complete time behavior of a burst excursion may be obtained only by numerical calculation, approximate analytical solutions can be found which are valid within limited regions. Thus, consider first the fission rate immediately after establishment of reactivity ρ_0 (with negligible initial neutron density) and before appreciable heating occurs. For this case, the appropriate solution early in the rise is

$$\dot{F} = \dot{F}(0)e^{\alpha t} \quad (3)$$

where α is the positive solution to the inhour-type equation

$$\frac{\alpha}{\alpha_R} = \rho_0 + \sum_{i=1}^6 \frac{a_i \lambda_i}{\lambda_i + \alpha} \quad (4)$$

[†] Contribution of the Doppler effect to temperature coefficient of reactivity is neglected since its effect in this case is indistinguishable from that of expansion. For highly intense bursts where expansion lags fission energy release, Doppler effect should be considered separately, but is beyond the scope of this paper.

For large initial reactivity, viz., where $\alpha \approx \rho_0 \alpha_R$, a burst solution is obtained readily by neglecting the delayed neutron contribution or last term of Eq. (2) giving the following expressions (Ref. 5 presents a more rigorous derivation):

$$\dot{F}(t) = 2 \rho_0 \alpha e^{\alpha t} / (1 + e^{\alpha t})^2 \quad (5)$$

$$\text{and} \quad F(t) = 2 \rho_0 e^{\alpha t} / (1 + e^{\alpha t}), \quad (6)$$

which are useful for time $t < 1/\lambda_i$ measured from time of maximum fission rate. Thus within given limitations of Eq. (2), the following properties of the excursions as represented by Eq. (5) may be stated:

- (a) Peak fission rate, $\dot{F}(0) \equiv \dot{F}_m = \frac{1}{2} \rho_0 \alpha$
- (b) Burst width at half-maximum, $t_w = 3.52 \alpha^{-1}$
- (c) Total fission yield, $F(\infty) \equiv F_T = 2 \rho_0$.

In addition, Eq. (6) reveals the reflection of excess reactivity [$\rho_0 - F(t)$] about prompt critical during a super-prompt-critical excursion.

The residual power level (see earlier) remaining after shutdown of the primary burst peak may be derived essentially by using the yield of the burst which precedes it as given by (c) for an initial condition in Eq. (2) for consideration of later times to obtain, for example, the following limiting functions:

$$\dot{F}(t > t_w) \simeq 2 \sum_{i=1}^6 a_i \lambda_i e^{-\lambda_i t} \quad \text{if } \rho_0 \gg 0, \quad (7)$$

$$\dot{F}(t > t_w) \simeq \sum_{i=1}^6 a_i \lambda_i e^{-\lambda_i t} \quad \text{if } \rho_0 \sim 0. \quad (8)$$

Thus, as might be expected, fission rate in this region should follow the characteristic decay of delayed neutron activity in a fissile sample following an impulse-type activation.⁶ Equation (8) suggests the correction term which added to (a) gives the first order solution for peak fission rate, which is

$$\dot{F}_m = \frac{\rho_0 \alpha}{2} + \sum_{i=1}^6 a_i \lambda_i \quad (9)$$

and applies even for negative values of ρ_0 .

In the region of high initial excess reactivity, the assumption $\rho(t) = \rho_0 - F(t)$ begins to lose validity, i.e., volume expansion begins to lag fission energy release. This may be expected to occur when the initial period or e -folding time, α^{-1} , approaches the time for pressure waves to travel through the assembly. A more rigorous treatment to include this effect is to write for $\rho(t)$ in Eq. (2) the expression [$\rho_0 - C_1 \Delta V(t)$] where C_1 is a constant and ΔV is volume dilation. Next, recourse is taken to the hydrodynamical equations of the assembly to obtain an equation relating ΔV and fission yield $F(t)$. Finally, the two equations are solved simultaneously. The procedure

is too lengthy to develop here, but results so obtained⁵ in the form of bounds are:

$$\begin{aligned} F(t) &< 2 \rho_0 (1 + \alpha^2 \tau^2) e^{\alpha t} / (1 + e^{\alpha t}), \\ F(t) &> \rho_0 (1 + \alpha^2 \tau^2) (1 - e^{-2\alpha t}), \end{aligned} \quad (10)$$

where τ is essentially the fundamental period of mechanical vibration for the assembly. To a first order of approximation, the inertial effect considered above increases the maximum fission rate and burst yield by the factor $(1 + \alpha^2 \tau^2)$. A lower limit on burst width also is predicted by (10), viz., $t_w > 2.44 \alpha^{-1}$.

Predictions developed in this section are compared graphically with experimental observations in the following section.

Experimental

The investigation of burst properties discussed here was part of a program⁷ to determine the behavior of supercritical systems for the evaluation of reactor hazards and also the hazards of less standard operations involving possibly critical configurations of active material. Results have been used, for example, as a basis for normalization of fast reactor accident calculations.⁸ The fact that observations presented were made on Godiva I rather than Godiva II facilitates comparison with features of the theory directly applicable to only spherical geometry. However, results presumably apply, with small but tedious modifications, to Godiva II bursts.

Observations made on each burst excursion studied included the following:

1. Initial reactivity was determined from calibrated control rod position combined with the known contribution from burst rod insertion.

2. Initial reactor period (α^{-1}) was measured from the trace of an oscillograph whose horizontal deflection responded to the output voltage from a scintillation detector mounted near the assembly, with sinusoidal waves of known frequency applied in vertical deflection for time calibration.

3. Total fission yield for the excursion was determined both from temperature rise as measured with a thermocouple imbedded in the assembly and also from the measured (n, p-induced) beta activity of a compressed sulfur pellet attached to the assembly surface. The integrated leakage neutron flux as determined from the sulfur was related to total fissions by previous calibration against a radiochemical determination of fissions produced in a small central uranium sample.

4. Over-all time behavior of power level was recorded using a large scintillation detector employing ~ 3 gallons of DPT (diphenylhexatriene in a saturated solution of terphenyl in toluene) viewed by a high-current photocell (RCA C7154). Placed about one meter from Godiva, this detector responded to both leakage neutrons and gammas with negligible contribution from room or ground scattering. Good photocell response linearity up to high currents justified its use in covering the five decades in power

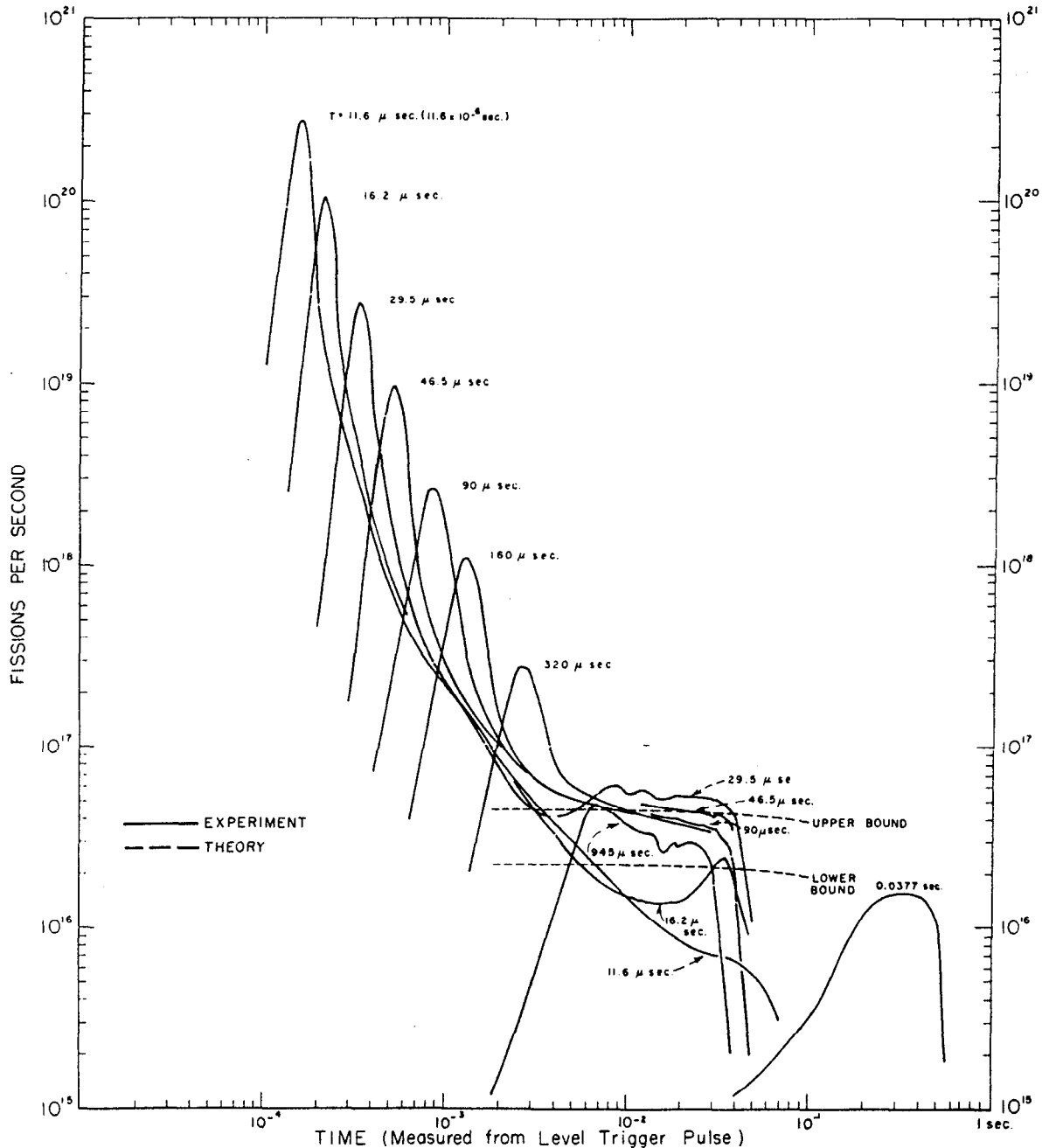


Figure 4. Complete excursions for different initial reactivities as indicated by the measured reactor period, $T = \alpha^{-1}$

level necessary for intense bursts. The procedure used to record this wide range was to connect the photocell output to the vertical amplifiers of four camera-equipped oscilloscopes each with a different amplification in addition to a different linear horizontal sweep speed to cover the necessary total of three decades on the time axis. Sweeps were simultaneously initiated by a radiation-level trigger which was generated by a very sensitive scintillation detector at a time early in the burst rise.

Some complete burst excursions are shown plotted with logarithmic coordinates in Fig. 4. Burst amplitude, originally obtained as an oscilloscope

deflection voltage, was converted to fissions per second by equating the integrated time-voltage area (from photographic presentation) of each excursion to the corresponding measured fission yield. Time is measured from radiation-level trigger time which was adjusted to occur roughly at the same amplitude for all bursts, with the result that wider bursts appear later in time than narrow, more intense, bursts. Termination or scram time appears in the neighborhood of 0.04 second for all bursts except the $T = 0.0377$ -sec excursion for which it was 0.5 second to allow for full burst development. The theoretical curves, shown as broken lines, are the upper and

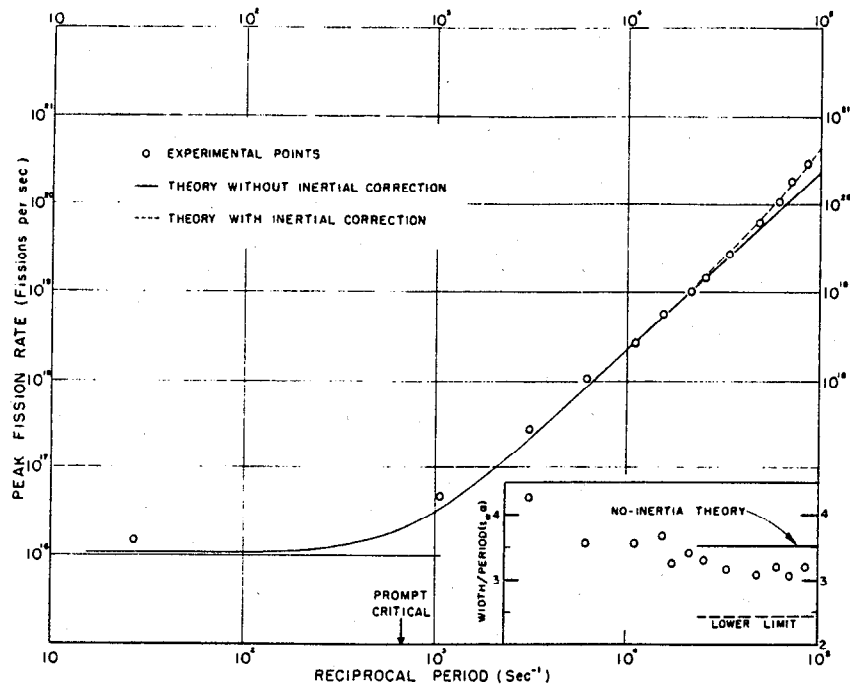


Figure 5. Maximum burst amplitude and width (normalized to reactor period) vs. α

lower bounds for residual level calculated from Eqs. (7) and (8) using appropriate delayed neutron parameters given in Ref. 6. While there is qualitative agreement between theory and experiment here, the observed residuals are generally higher than predicted, which may be attributed either to a systematic experimental error or to the use of incorrect delayed neutron parameters in the calculations. (For example, all γ_i were assumed equal whereas the use of larger values for the short-period groups would reduce the discrepancy.) For the most intense bursts, pressure waves in the assembly were sufficiently intense to separate momentarily the assembly components immediately after the primary burst. The resultant drop in reactivity is observed as a drop in the residual amplitude, as may be seen in the figure, and for the $T = 11.6 \times 10^{-6}$ -sec burst, recovery does not occur before scram time.

Maximum amplitudes attained during observed excursions are shown as experimental points in Fig. 5, together with measured burst width at half-maximum, plotted against reciprocal initial reactor period. While initial excess reactivity is considered the independent variable in determination of burst characteristics, the observed scatter in its experimental evaluations was found to be greater than in measurements of the associated initial reactor period (see Eq. (4)). Accordingly, graphical data presentation is improved by using reciprocal period in place of initial reactivity. The solid theoretical curve for peak fission rate was calculated using Eq. (9) with 4.8×10^{16} fissions per dollar, an empirical conversion coefficient obtained as the product of the measured temperature coefficient of reactivity and fission yield per degree temperature rise—measure-

ments discussed in item 3 above. The broken curve was calculated by multiplying the right-hand side of Eq. (9) by $(1 + \alpha^2\tau^2)$ with τ taken as 10^{-5} second. Upper and lower bounds for burst width as shown in the inset of Fig. 5 are predictions from Eqs. (5) and (10), respectively.

For the purpose of comparing results with theory, fission yield in the residual level is subtracted from measured total excursion yield to give total fissions in the primary burst peak, which is shown plotted against α in Fig. 6. The solid curve is a prediction from Eq. (6); the broken curve was calculated by multiplying this by $(1 + \alpha^2\tau^2)$. In such calculations, reactivity ρ_0 was obtained from Eq. (4) (see plot in Fig. 7) with $\alpha_R = 1.09 \times 10^6 \text{ sec}^{-1}$ as independently determined by J. D. Orndoff (Ref. 4 discusses such

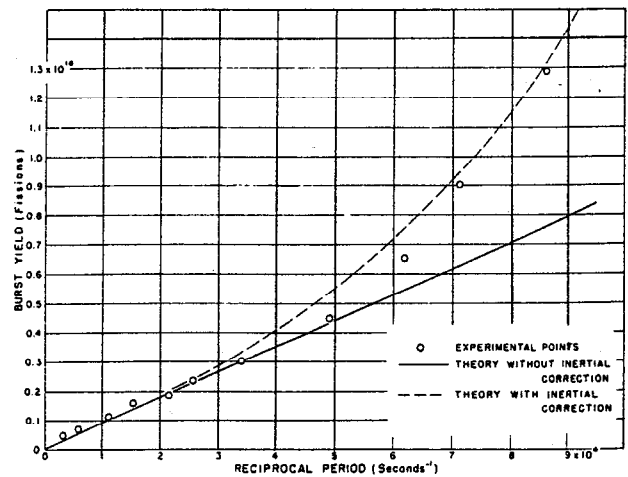


Figure 6. Total fissions occurring in primary burst vs. α

determinations and gives a slightly smaller result for Godiva I obtained under different experimental conditions).

Total prompt-burst yield has been limited to about 10^{16} fissions, under controlled conditions, to prevent possible rupture of the uranium metal. Estimations by G. E. Hansen⁵ indicate internal pressures (or consequent surface tensions) to be ~ 1500 atmospheres for this yield in Godiva I, whereas tensions of ~ 5000 atmospheres exceed the tensile strength of uranium.

INVESTIGATIONS OF DELAYED RADIATIONS FROM FISSION

Delayed Neutrons

A comprehensive investigation of delayed neutron parameters has been completed at Los Alamos⁶ using Godiva I as the neutron source for sample activation. The periods, relative abundances, and absolute yields of delayed neutrons from both thermal and "fast" fission of U^{235} , U^{233} and Pu^{239} , and from fast fission of U^{238} , Pu^{240} and Th^{232} , were measured. The "fast" (fission spectrum) irradiations were made in the center of Godiva, and the thermal-fission irradiations were made in a large (cadmium shielded) polythene block mounted near Godiva. Delayed critical and prompt-burst irradiations were used to emphasize the longer- and shorter-period contributions, respectively.

Equation (4) (the "inhour equation") has been evaluated using the appropriate delayed neutron data for Godiva, obtained from Ref. 6. The resulting plot of Eq. (4) in the region of prompt critical

is compared in Fig. 7 with experimentally observed reactor periods obtained during the burst studies (section on Burst Generation). The excellent agreement in Fig. 7 between the calculated curve and measured points provides a sensitive check on short-period delayed neutron data, and also indicates negligible contribution from possible shorter-period groups.

Delayed Gammas

A study of time dependence and energy spectra of delayed gammas from several different fissile elements is currently in progress using Godiva II as the neutron source. A sample which has been activated in the assembly is pneumatically transferred (as in delayed neutron experiments) to a shielded 4×4 -in. NaI-crystal detector. Some preliminary observations (uncorrected except as indicated) using 0.1 g U^{235} are presented in Figs. 8 and 9. The data for Fig. 8 were obtained after activation by a burst producing a peak assembly temperature rise $\sim 10^\circ C$ or $\sim 1.5 \times 10^{15}$ fissions, i.e., this was a flat-topped excursion 0.04 second in length corresponding in amplitude to the region just below prompt critical in Fig. 5. Time decay was monitored using a multichannel recording time-delay analyzer.⁹ An interesting feature of these data is that decay varies as t^{-k} over the last three decades observed, with k less than unity instead of greater than unity as usually reported.¹⁰ This may be due in part to the short activation time and/or the choice of energy threshold. A burst of 10^{16} fissions activated the sample for pulse-height data presented in Fig. 9. The assembly excursion was therefore similar to that of the $T = 29.5 \times 10^{-6}$ -sec burst shown in Fig. 4. Data were accumulated in a 100-channel

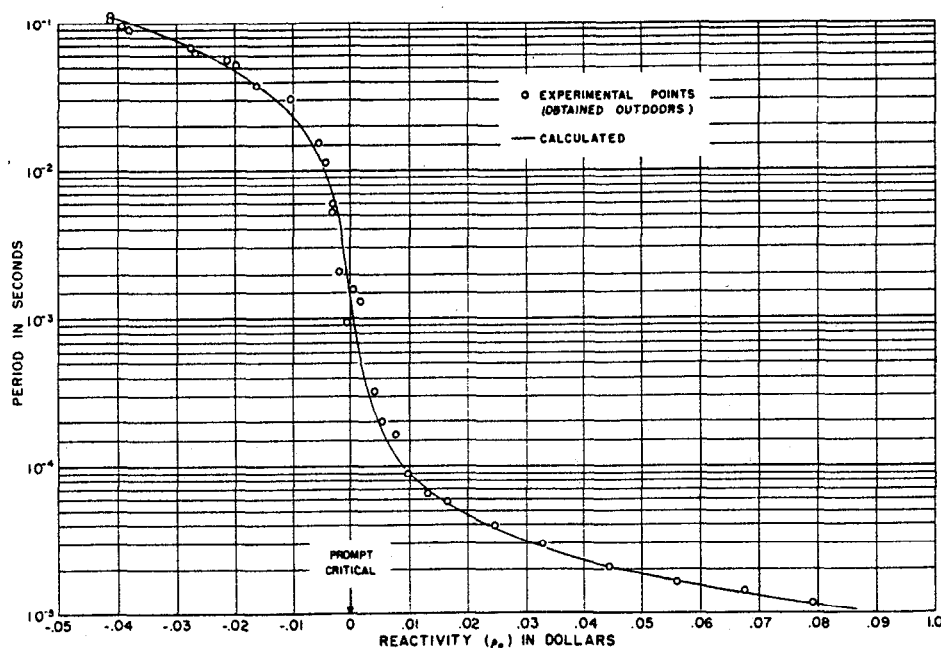


Figure 7. Godiva period α^{-1} vs. reactivity ρ_0 in the region of prompt critical. The solid curve is calculated from Eq. (4); points were measured periods. To minimize effects of roomscattered neutrons, the data were taken with the assembly suspended 26 feet above ground outdoors

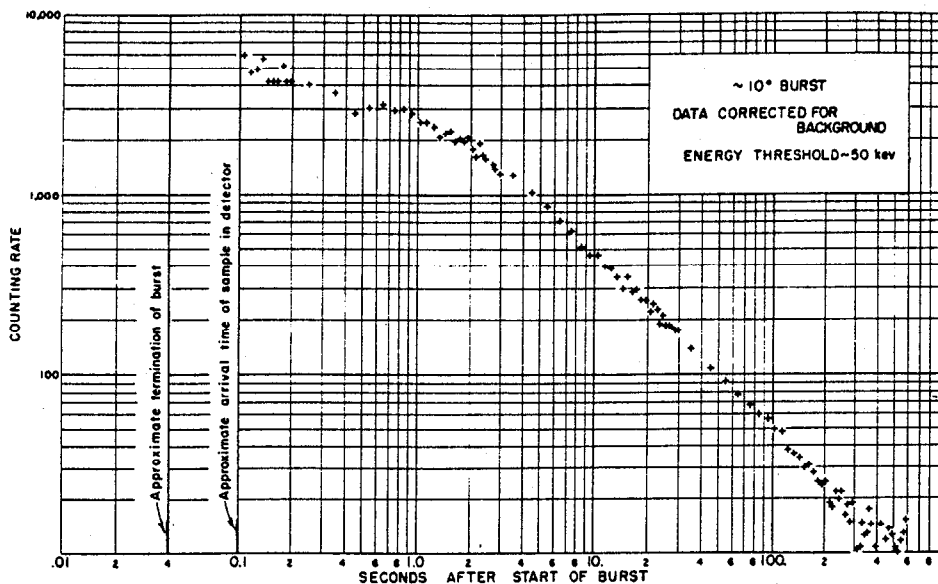


Figure 8. Time decay of fission gammas from U^{235} sample after activation (~ 0.04 sec) producing 6×10^8 fissions. Data are uncorrected except for background

pulse height analyzer over the time interval between 1 and 3 seconds after burst time.

SURVEY OF SHORT-LIVED GAMMA OR BETA ACTIVITIES

As demonstrated by results discussed in the preceding section, Godiva neutron bursts supplemented by delayed critical irradiations are particularly useful for activations involving half-lives from 0.05 to 100 seconds. It is therefore planned to use Godiva II in a comprehensive survey of neutron-induced gamma or beta activity in nonfissionable elements with half-lives in this region. By utilizing the high available time-integrated flux density ($int \sim 10^{14}$ neutrons/cm² per burst at the center), the survey will include elements with very low reaction cross sections. The experimental setup (see "Delayed Gammas") for studying time decay of fission gammas will be employed in this program with only slight modification.

BIOLOGICAL EFFECTS OF DOSAGE RATE

The Godiva assemblies are uniquely applicable in studies of biological dose rate effects. Not only can equal doses be delivered in times from 10^{-4} second (burst) to several minutes, but also the degraded fission neutron spectrum¹¹ is relatively uncontaminated with gamma rays. (The dose ratio of neutrons to gammas is about 7:1.) Following are examples of biological dose rate studies, utilizing Godiva I or II, which are completed or in progress:

1. Haploid yeast cells (*Saccharomyces cerevisiae*) and basic biochemical unit DNA (desoxyribose nucleic acid). These were exposed to doses from 500 to 10,000 rad (one rad corresponds to 100 ergs/g energy deposition in soft tissue), and the end points recorded were death or functional inactivation. In either biological system no significant dose rate effect

has been noted to date, within the biological experimental error (15–20%), in the range 10^2 to 10^{10} rad/min.

2. Broad bean root (*Vicia faba*). Sensitive root tips of this plant have been exposed thus far only to long irradiations. From these exposures, the RBE (relative biological effectiveness in causing death of the root) for Godiva II radiation was found to be ~ 10 times that of a Co^{60} source, which may be compared with RBE of 2–3 for acute end points in mammalian systems.

3. Mammals. Studies on mice (interrupted by a virus infection) covered a dose range from 50 to 500 rad and included measurements of spleen and thymus weight loss at 5 days post-exposure. Rates were varied from 10^1 to 10^3 rad/min, and again no significant rate effect was observed. Doses of greater than 5000 rad were studied using mean survival time in mice as the end point of effect—again with negative results. Similar results were obtained on monkeys at dose rates from 10^3 to 10^{10} rad/min.

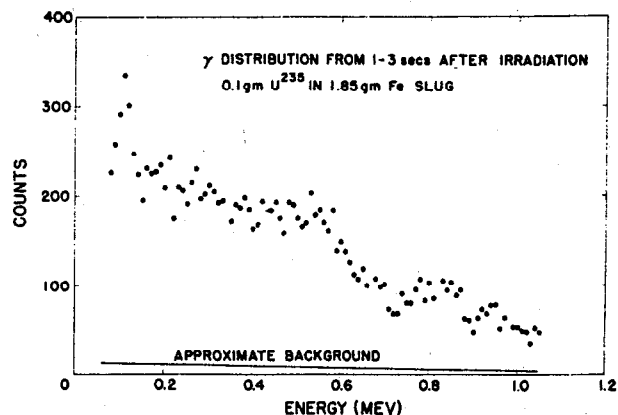


Figure 9. Energy spectrum of delayed gammas (uncorrected data) in time interval between one and three seconds after burst activation which produced 4×10^{10} fissions in the sample

TRANSIENT RADIATION EFFECTS ON ELEMENTARY MATERIALS

It is a reasonably established fact that the passage of a sufficiently energetic particle through a crystal lattice creates, along the trajectory of the particle, a region of radiation damage which consists of vacancies and interstitial atoms, and possibly more extensive lattice disruption. The regions of disrupted lattice affect some of the gross crystal properties; e.g., the elastic constants will change and the electrical resistivity may increase. The study of transient effects associated with such damage is a relatively unexplored field of application for which Godiva bursts are ideally suited. The requirement of enormous doses for observable effects is one reason why this field is so untouched. In semiconductors, for example, no damage is observed below a time-integrated neutron flux density $nvt \sim 10^{12}$ neutrons/cm². Using Godiva II bursts, samples placed adjacent to the wire cage (seen in Fig. 2) may receive an integrated flux density of 2×10^{13} neutrons/cm² with a peak rate $nv \sim 2 \times 10^{17}$ neutrons/cm² sec, and small samples placed in a cavity near the center of the assembly receive about ten times these values.

The following are examples of burst applications, in studies of dose rate or transient effects in various materials, which are in progress or planned:

(a) *Semiconductors.* In work to date on transistors and crystal diodes, conductivity observations indicate permanent damage produced by bursts to be similar to that produced by long irradiations of equal total dose. However, by using bursts, some additional information is being obtained, such as determinations of recovery processes which may lead to better understanding of radiation damage in semiconductors. For example, Fig. 10 is a plot of conductivity versus time after burst exposure of an n-type germanium sample in an experiment being conducted by Stein and others of Sandia Corporation. They are also measuring hole-carrier lifetimes and transient photoconductivity during and immediately after irradiation. It is tempting to assume that the early decrease in conductivity shown in Fig. 10 is fall-off in gamma activity at the sample and that the later (~ 15 minutes) rise may be attributed to annealing effects.

(b) *Metal crystals.* Because radiation damage in metal crystal lattices is similar to that in semi-

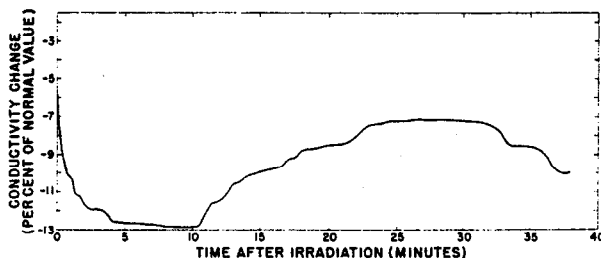


Figure 10. Conductivity of n-type germanium vs. time after burst irradiation. The sample ($20 \times 5 \times 5$ mm³) was exposed to $\sim 10^{13}$ n/cm² as determined from a nickel foil monitor

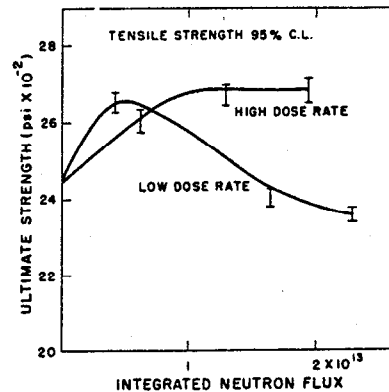


Figure 11. Tensile strength of Teflon as a function of time-integrated neutron flux. The two dose rates were obtained by varying the sample distance from Godiva II

conductors, an interpretation of resulting resistivity variations may also shed some light on the detailed mechanism of damage in metals. Accordingly, an experimental program similar to that in (a) has been organized by Levy of Brookhaven National Laboratory to investigate radiation damage in polycrystalline wire (and eventually in single metal crystals) by observing resistivity transients produced by neutron bursts from Godiva II. No actual irradiations have been performed as yet but it is hoped first to determine the total number of lattice defects formed per fission neutron recoil, then to determine the kinetics of the subsequent annealing process.

(c) *Plastics.* A large number of different plastics or elastomers have been exposed to Godiva bursts. These include rubber, Teflon (a fluorinated hydrocarbon), Plexiglas (polymethyl methacrylate resin), and nylon. Observations were made on such properties as hardness, tensile strength, elongation, stress-strain, and optical transmittance. Some results of these tests have been reported by Newell of Convair.¹² An example of a probable dose-rate effect which has been observed is presented in Fig. 11 showing a steady increase in tensile strength for Teflon with total radiation dose for bursts (high dose rate curve) compared with an increase followed by a decrease for low dose rate. This increase in strength is generally attributed to cross-linking between the long-chain molecules due to dislocations of certain atoms by fast neutrons. If indeed there is a rate effect here, a possible explanation would be that recombination is accelerated by the high instantaneous density of dislocations and defects produced by the burst.

EXAMINATION OF MONITOR RESPONSE IN CRITICALITY ACCIDENTS

Godiva II bursts have been utilized in formulating criteria for the monitoring of uranium-processing areas for criticality accidents, and to evaluate the detection range and reliability of several kinds of radiation detectors. Monitors tested included the Victoreen Remote Area Monitoring System employing both air- and BF₃-filled ion chambers, a NaI scintillation

monitor, and the Victoreen Model 350M Geiger-tube gamma monitor. Operation was observed at distances up to 1000 feet of air plus 15 inches of concrete using "standard" bursts of $\sim 10^{16}$ fissions. Results indicated, for example, a proven range for the BF_3 monitor of twice that for the gamma detectors. Blocking or saturation was observed only in some of the Geiger-tube monitors, but the use of latching relays was found to prevent the early opening of alarm circuits. On the basis of range-sensitivity

measurements, criteria have been formulated for the spacing and sensitivity of area monitors so that no person in a monitored area can receive more than a specified total radiation dose without an alarm being sounded.

As a result of such experiments, 70% of the Geiger-tube monitors have been eliminated at some Oak Ridge plants and sensitivity reduced on others with consequent improved safety and considerable savings in maintenance.

REFERENCES

1. R. E. Peterson and G. A. Newby, *An Unreflected Uranium-235 Critical Assembly*, Nuclear Sci. and Eng., **1**, 112 (1956); H. C. Paxton, *Critical Assemblies at Los Alamos*, Nucleonics, **13**, No. 10, 48 (1955). Prompt bursts were obtained earlier in the "Dragon" assembly of O. R. Frisch *et al.*, which is described in F. de Hoffman, B. T. Feld and P. R. Stein, *Delayed Neutrons from U-235 after Short Irradiation*, Phys. Rev., **74**, No. 10, 1330 (1948). However, the chain reaction was quenched by the mechanical separation of components rather than by self-limiting action.
2. *Godiva Wrecked at Los Alamos*, Nucleonics, **15**, No. 4, 104 (1957).
3. H. Hurwitz Jr., *Derivation and Integration of the Pile-Kinetic Equations*, Nucleonics, **5**, 61-67 (July 1949).
4. J. D. Orndoff, *Prompt Neutron Periods of Metal Critical Assemblies*, Nuclear Sci. and Eng., **2**, No. 4, 450-460 (1957).
5. G. E. Hansen, *Burst Characteristics Associated with the Slow Assembly of Fissionable Materials*, Los Alamos Scientific Laboratory Report, LA-1441 (1952); K. Fuchs, *Efficiency for Very Slow Assembly*, Los Alamos Scientific Laboratory Report, LA-596 (1946).
6. G. R. Keepin, T. F. Wimett and R. K. Zeigler, *Delayed Neutrons from Fissionable Isotopes of Uranium, Plutonium and Thorium*, J. Nuclear Energy, **6**, 1-21 (1957); Phys. Rev., **107**, No. 4, 1044-1049 (1957).
7. T. F. Wimett, *Time Behavior of Godiva Through Prompt Critical*, Los Alamos Scientific Laboratory Report, LA-2029 (1956).
8. R. O. Brittan, *Some Problems in the Safety of Fast Reactor Calculations*, ANL-5577 (1956); W. R. Stratton *et al.*, *Analysis of Prompt Excursions in Simple Systems and Idealized Fast Reactors*, private communication.
9. P. G. Koontz, C. W. Johnstone, G. R. Keepin and J. D. Gallagher, *New Multichannel Recording Time-Delay Analyzer*, Rev. Sci. Instr., **26**, 546-554 (1955).
10. J. M. Wyckoff and H. W. Koch, *Delayed Gammas from Uranium Photofission*, Natl. Bur. Standards Report No. 4335 (1955).
11. G. M. Frye, J. H. Gammel and L. Rosen, *Energy Spectrum of Neutrons from Thermal Fission of U-235 and from an Untamped Multiplying Assembly of U-235*, Los Alamos Scientific Laboratory Report, LA-1670 (1954).
12. D. M. Newell, *Irradiation of Plastics at Godiva*, Paper presented at the WS 125A Radiation Effects Symposium (October 1957), Convair-Fort Worth Report FZM 1028 (1958).

Mr. Wimett presented a summary of Papers P/419, P/1848 and P/2364 at the Conference and added the following comments:

For many experimental applications where extremely high flux densities are needed but relatively low total energy release, pulsed reactors with their negligible cooling requirements provide a convenient solution. I shall discuss examples of pulsed or fission burst facilities, specifically those which are solid and homogeneous, with emphasis on their relative merits with regard to experimental application.

The first requisite of a pulsed reactor is that the temperature coefficient of reactivity be negative or that some infallible intrinsic shutdown mechanism exist which will prevent excessive runaway power excursions. Mechanical scrams are generally too slow to check energy release associated with the very short reactor periods involved.

Perhaps the simplest kind of intrinsic self-regulation is that found in a bare fast reactor such as Godiva I

or its successor, Godiva II, which is now in operation at Los Alamos. In this case, it is thermal expansion, which is linearly proportional to energy release within limits, that provides the shutdown mechanism. Of course, the Doppler effect tends to oppose this shutdown because of a high U^{235} enrichment but produces a much smaller effect. Long experience with these reactors has demonstrated the expansion mechanism to be highly reliable as attested to by the rather modest damage produced during the extreme unplanned power excursion of Godiva I which led to its retirement. In addition to other more complex self-limiting mechanisms such as have been demonstrated under pulsed conditions in the water-moderated class including BORAX, SPERT and KEWB, there has been proposed a new mechanism which applies to solid, homogeneous, moderated reactors. None have been operated under burst conditions as yet, but theory predicts a temperature coefficient to arise from direct coupling between power level and the thermal neutron energy distribution in such systems.

Two design proposals which rely on this phenomenon are reported—one by Freund, Iskandarian and Okrent, of Argonne National Laboratory in Paper P/1848, a second by McReynolds, Stein and Taylor, of General Dynamic Corporation, in Paper P/2364. The two very similar designs are called TREAT and FLASH respectively, and employ a dispersion of enriched uranium oxide in graphite as the core matrix.

Turning now to performance and research applications, one of the first uses made of Godiva I was to determine the behavior of fast supercritical systems for evaluation of reactor hazards. For this purpose a series of power excursions initiated by sudden reactivity additions was instrumental and yielded response information for excess reactivities extending from delayed critical to one-tenth dollar above prompt critical. The results so obtained compare satisfactorily with calculations based on the Fucks-Hansen model, for example, as may be seen in Fig. 5, P/419, which shows a graph of maximum fission rate plotted against reciprocal initial reactor period as measured early in the excursions. Scales on both axes are logarithmic. Circles are experimental points taken from the maximum power amplitude of the burst excursion; the solid line is predicted from theory neglecting inertia of the expanding system; the dotted curve includes a first order inertial correction. In the lower right-hand corner, the ordinate is burst width in units of initial reactor period and the observed widths are seen to approach three reactor periods as reciprocal period increases toward 10^5 reciprocal seconds, which is midway between the predictions with and without inertial corrections.

Notice that observed peak fission rate at the upper end is in the neighborhood of 3×10^{20} fissions per second or 10,000 megawatts which is taken as an upper limit dictated by 100°C maximum allowable temperature rise. I would like also to call your attention to the flat region of the curve, which obtains for reciprocal periods less than the value corresponding to prompt critical reactivity. What happens in this region is that no actual fission pulse is developed; the power simply rises, levels off, and begins to decay at a rate determined by the delayed neutron activities, all of which have decay constants longer than the initial reactor period in this region. Thus, one has nearly steady operation here at a reproducible power level which is nearly independent of initial reactivity. Of course, Godiva must be scrambled within about one or two seconds to avoid overheating because, even here, the level is about 0.3 megawatt. Nevertheless it provides a convenient means for achieving intermediate irradiation times, for example, which may be used to selectively activate radio-isotopes with mean lives in the vicinity of one second.

From the time when fission pulse generation was first demonstrated on Godiva I, there has been an increasing demand for neutron pulse irradiations at LASL. Godiva I pulses were essential in activating fissile samples for the comprehensive investigation of delayed neutron parameters which was completed

at Los Alamos. The periods, relative abundances and absolute yields of delayed neutrons from both thermal and fast fission of U^{235} , U^{233} and Pu^{239} and from fast fission of U^{238} , Pa^{240} and Th^{232} were measured.

A number of biological experiments to study dose rate effects have been completed or are in progress using Godiva II bursts. For this purpose the Godiva leakage spectrum is particularly useful not only because it is fast but also because there is little contamination with gamma rays. Neutron dose is about seven times gamma dose. Yeast cells, broad bean roots, mice and monkeys have been irradiated on Godiva II.

Another field of application which has been practically untouched is that of radiation damage studies on elementary materials. To produce damage such as lattice deformation, energetic particles are necessary and for transient studies short pulse activation is ideal.

For inducing measurable lattice damage in semiconductors, for example, about 10^{12} fast neutrons per square centimeter is required. Using Godiva II bursts, samples placed just outside the wire cage receive twenty times this during a standard conservative burst and small samples placed in the central cavity are exposed to flux integrals another order of magnitude higher. In addition to semiconductors, many plastics and elastomers have been irradiated, and a program for studying radiation annealing in metal crystals is planned for Godiva II.

Godiva II bursts have also been utilized in formulating criteria for the monitoring of uranium processing areas for criticality accidents and to evaluate the detection range and reliability of several kinds of radiation detectors.

Regarding applications of TREAT and FLASH, there should be little overlap with those of Godiva for several reasons. First, pulse length will be longer by at least a factor of a thousand due to longer neutron lifetimes. Secondly, the useful flux will be nearly thermal. Thirdly, the source will be much larger, hence more useful in irradiating bulky objects.

Thus, TREAT will not be as applicable for lattice radiation damage studies nor for activating threshold

Table 1

	TREAT	GODIVA
Nominal core size	$1.5 \times 1.5 \times 1.2$ m	17.5 cm diam.
Uranium loading (kg U^{235})	11.2	54
Energy release (Mw-sec)	1000	0.35
Prompt neutron mean life (sec)	8.6×10^{-4}	6×10^{-9}
Maximum hot spot core temp.	400°C	150°C
Minimum reactor period (sec)	4×10^{-2}	10^{-5}
Average flux field (<i>not</i>)	3.4×10^{15}	2×10^{14}
Peak flux (core average) (<i>not</i>)	2×10^{16}	2×10^{18}
Peak power (Mw)	5×10^3	10^4
Cooling time (hours)	~ 5	0.5

fissioners but excellent for meltdown studies on uranium or plutonium fuel elements because of the very large flux integral obtainable. For radiation therapy, activation analysis, radioisotope production, and reactor technology, it should be invaluable.

To better compare and summarize some design features, Table I gives comparable details roughly calculated for TREAT and Godiva. Because of its intermediate size, similar features for FLASH should fall somewhere between these two sets of data.